Research Article

Received: 31 December 2015 Revised: 10 June 2016 Accepted article published: 15 July 2016 Published online in Wiley Online Library: 4 August 2016

(wileyonlinelibrary.com) DOI 10.1002/pi.5199

Elastomeric ethylene copolymers with carbon nanostructures having tailored strain sensor behavior and their interpretation based on the excluded volume theory

Humberto Palza,* Cristhian Garzon and Mauricio Rojas

Abstract

Two ethylene/1-butene thermoplastic elastomer copolymers were melt mixed with either multiwalled carbon nanotubes (CNTs) or thermally reduced graphite oxide (TrGO) resulting in piezoresistive composite materials. The effect of the polymer matrix, carbon nanostructure and filler concentration on the electrical behavior of the sensors was analyzed. The percolation process confirmed the relevance of these parameters as different thresholds were found depending on both the matrix and the filler. For instance, composites based on TrGO presented higher percolation thresholds than those based on CNTs. Regarding the strain sensor behavior of the electrically conductive composites, by using a matrix with a low amount of 1-butene comonomer, higher resistance sensitivities were observed compared with the other matrix. Noteworthy, composites based on TrGO filler presented strain sensitivities one order of magnitude higher than composites based on CNT filler. These results are explained by the excluded volume theory for percolated systems. Based on these findings, polyethylene piezoresistive sensors can be designed by a proper selection of polymer matrix, filler concentration and carbon nanoparticles.

Keywords: carbon nanofillers; piezoresistive materials; thermoplastic elastomers; nanocomposites; excluded volume theory

INTRODUCTION

One of the best routes to take advantage of the outstanding properties of carbon nanostructures is by their mixing with polymer matrices overcoming some limitations of macromolecules such as low mechanical performance and low conductivity.[1,2] These polymer nanocomposites are therefore ideal candidates for the fabrication of multifunctional materials extending the range of application of commodity plastics, such as polyethylenes (PE). In particular, by adding low concentrations of these carbon nanomaterials into a polymer matrix, a three-dimensional network can be formed producing a percolation transition where composites increase their electrical conductivity by several orders of magnitude. These conductive composites can be used in several fields such as in sensors[2] by taking advantage of their piezoresistivity, i.e. the variation of the electrical resistivity when a strain is applied. In these applications, sensitivity is one of the most important characteristics tailored by a broad range of parameters such as filler loading, matrix type and film fabrication method.[3,4] From the bioengineering point of view, polymer composites with piezoresistivity can be applied in human knee flexion/cyclic movement for orthopedics and rehabilitation or in applications related to human epidermis.[5–7]

Although films of either carbon nanotubes (CNTs) or graphene deposited on polymer surfaces are relevant for piezoresistive sensors,[8–10] composites based on embedded carbon nanostructures are also a good alternative. In the latter case, multiwalled CNTs are the most common carbon based filler. For instance, styrene-butadiene-styrene elastomers with different compositions were mixed with CNTs for sensor applications at large strain obtaining high sensitivities.[11] The electromechanical sensitivity in this case depended on the butadiene contents with softer matrices displaying larger changes. This sensitivity was quantified by the gauge factor (GF), which is defined as the slope between the relative changes in electrical resistance with the applied mechanical strain. In this case, a maximum in the GF around 30 at strains around 20% was obtained; meanwhile a GF varying between 2 and 8 was found at 5% of strain further depending on the filler concentration.[5,11] Composites close to the percolation threshold showed larger values of GF. Polyurethane thermoplastic elastomers having a network of entangled CNTs were also tested for piezoelectric applications showing electrical resistance increases up to 270 times at elongations as high as 400%.[5] Similar thermoplastic polyurethane/CNT composites presented piezoresistivity with good recoverability and reproducibility after cyclic loading stabilization although at low strains.[12] At large strains only a small part of the resistivity is recovered. Polyvinylidenefluoride mixed with CNTs also displayed a sensitive network able to monitor the strain levels in materials.[13] Polymer blends can also be developed in this context such as

* *Correspondence to: H Palza, Departamento de Ingeniería Química y Biotecnología, Facultad de Ciencias Físicas y Matemáticas, Universidad de Chile. E-mail: hpalza@ing.uchile.cl*

Departamento de Ingeniería Química y Biotecnología, Facultad de Ciencias Físicas y Matemáticas, Universidad de Chile

those based on styrene-butadiene-styrene and thermoplastic polyurethane mixed with CNTs.[3] In this case, piezoelectric composite sensors with stronger interaction and poorer dispersion showed the highest sensitivities. A mix of CNTs and carbon black embedded in thermoplastic elastomer polyurethanes can be further used in these applications.[14]

Despite the good behavior of polymer/CNT piezoelectric composite sensors, similar to other applications, nowadays there is a strong tendency to replace high cost CNTs by graphene based materials.[15] In particular, strain sensors based on polymer composites with graphite derivatives have been developed although focused mainly on the pressure effect.[16,17] High density PE mixed with graphite nanosheets by two-roll mixers showed a sharp positive pressure coefficient of resistivity with changes as high as two orders of magnitude.[17,18] In this case, piezoresistivity depended on the morphology, spatial arrangement and concentration of filler, as concluded by analyzing two carbon fillers at different concentrations. A critical pressure threshold, below which composite resistance decreased with increase of pressure and above which resistance increased sharply with increase of pressure, was observed. In similar PE/exfoliated graphite composites, the piezoresistivity strongly depended on time.[19] Silicone rubber with graphite nanosheets also presented a sharp positive pressure coefficient effect of the resistivity although at very low pressure.[20] Acrylonitrile-butadiene rubber compounds filled with different concentrations of graphite nanoplatelets changed their electrical conductivity by more than five orders of magnitude upon a 60% compression.[21] Isobutylene-isoprene copolymers filled with two different graphite derivatives, namely reduced graphene oxide and expanded graphite, were also studied for piezoresistivity sensors.[22] The relative resistance of the composites decreased with pressure and, unlike expanded graphite filler, the electrical resistance of the composites with reduced graphene oxide filler changed regularly with uniaxial pressure due to the large number of contacts between particles.

The piezoresistivity observed in these strain sensors based on polymers with carbon nanostructures is usually well explained by changes in both the carbon network and the interparticle distances as stated by tunneling theory.[20,23–25] This tunneling effect means a nonlinear relationship between electrical resistance and strain, especially at low CNT concentrations and high strains. Moreover, it can explain why composites near the electrical percolation threshold present larger electromechanical sensitivities than those above the percolation threshold due to the high variation of the carbon network with strain and therefore of the electrical resistance.[11,26] For instance, experimental results showed that, when the CNT loading approaches the percolation threshold, the GF of the polymer composite sensors increases remarkably.[26] The particle aspect ratio is another relevant parameter to evaluate the strain sensor behavior[18,23] and, for nanocomposites based on CNTs, a nearly linear dependence of resistance *versus* strain was observed, whereas spherical carbon black based nanocomposites exhibited a more exponential dependence.[23] The aspect ratio effect is explained by the morphology of the conducting network (number of contacts, contact orientation etc.). For instance, the number of interparticle tunneling contacts along a conductive pathway is significantly higher in the case of spherical fillers whilst tube-like fillers present a more redundant network structure as they can be in electrical contact with numerous other CNTs.[23]

Regarding the polymer matrix, the development of piezoelectric sensors based on thermoplastic elastomer polymers is highlighted as this kind of matrix allows the combination of the mechanical properties of rubber with the processability and recyclability of thermoplastics. Examples of these matrices, as above mentioned, are styrene-butadiene-styrene, acrylonitrile-butadiene copolymers and thermoplastic polyurethanes. However, despite the industrial relevance of PE based materials, to our knowledge the thermoplastic elastomer PE has barely been studied for piezoresistive nanocomposites. Here, we introduce a study about piezoresistive polymer/carbon nanostructured composites based on the thermoplastic elastomer PE because of its exceptional performance associated with good control over polymer structure, molecular weight distribution, uniform comonomer composition and rheology.[27] These PEs are ethylene-olefin copolymers synthesized by single site catalysts allowing perfect topological control and therefore facilitating studies about the relationship between microstructure and the final properties of the polymer. To our knowledge only carbon black fillers have been used for piezoresistive thermoplastic elastomer PE.[28,29] The aim of our contribution was to study the piezoresistive behavior of two thermoplastic elastomer ethylene copolymers by using either CNTs or graphite derivatives as fillers focusing on the effect of the polymer matrix and carbon nanostructure.

EXPERIMENTAL

Two commercial grade ethylene-1-butene copolymers from Dow Chemical (Midland, MI, USA) were used as the polymer matrix, named EB1 (commercial code HM7289) and EB2 (commercial code HM7387). Based on the datasheet information provided by Dow, the densities, the total crystallinity, the melting temperatures and the flexural modulus are 0.891 and 0.870 g cm^{-3}, 28% and 16%, 99 and 50 °C, and 43.5 and 11.5 MPa for EB1 and EB2, respectively. From this information, a higher incorporation of 1-butene in EB2 than EB1 is concluded based on the relationship between comonomer content and both crystallinity and melting temperature.[27,30] Moreover, on the basis of experimental results from similar copolymers, the comonomer content can be roughly estimated at around 6 and 14 mol% for EB1 and EB2, respectively.

Extra pure graphite powders (G), sulfuric acid (98.08%, H_2SO_4), potassium permanganate (99%, $KMnO_4$), hydrochloric acid (32%, HCl) and sodium nitrate (99.5%, $NaNO_3$), were obtained from Merck (Germany) and used as received. Hydrogen peroxide (5%, H_2O_2) was purchased from Kadus S.A. Thermally reduced graphite oxide (TrGO) was prepared in a two-step oxidation/thermal reduction process using G as raw material. The graphite oxidation process of Hummers and Offeman was employed as detailed elsewhere.[31,32] The first step was oxidation of G with $KMnO_4$ and $NaNO_3$ in concentrated sulfuric acid obtaining graphite oxide (GO). In a second step, the dry GO was thermally reduced to afford TrGO by rapidly heating GO in a nitrogen atmosphere to 600 °C during 40 s using a quartz reactor heated in a vertical tube furnace. Multiwall CNTs (Baytubes C150P) were obtained from Bayer Material Science AG (Germany). Based on the datasheet information provided by Bayer, they are characterized by a purity higher than 95 wt%, number of walls between 2 and 15, an outer mean diameter of 13–16 nm, an inner mean diameter of 4 nm, length between 1 and >10 μm, and a bulk density around 150 kg m^{-3}.

The composites were prepared by using a Brabender Plasticorder (Brabender, Germany) internal mixer at 170 °C and a speed of 110 rpm. Filler content ranged from 0 to 10 vol% for TrGO or CNTs. First, half the polymer and an antioxidant were added to the mixer operated at 110 rpm. After approximately 2 min to melt the polymer, the filler was added during 3 min. Finally, the rest

of the polymer pellets were added and the speed of the mixer was held at 110 rpm for 10 min. Therefore the total mixing time was around 15 min. Afterwards, the samples were press molded at 170 °C and 50 bar for 5 min and cooled under pressure by flushing the press with cold water, in order to obtain the final samples for tests. The samples were cut with a stainless steel mold with dimensions according to type IV (ASTM D638), i.e. bone type specimens with an overall length of 120 mm, distance between grips of 80 mm, width of narrow section 11.5 mm and thickness 1 mm. After sample preparation, the materials were left at room temperature for at least 3 days allowing crystallization of the highly amorphous polymer by annealing.

For the electrical resistivity/conductivity, different megohmmeters (Megger BM11 with a highest voltage of 1200 V and AEMC 1060 with a highest voltage of 5000 V) were used depending on the conductivity of the samples. With this set-up the standard two-point method was used. In this case, the electrodes were embedded into the samples for a bulk measurement. For each electrical value displayed in this work, at least four samples were prepared and four measurements for each one were carried out. In general, differences around one order of magnitude were detected in the non-percolated samples having low conductivity values (*ca* 10^{-9} S cm^{-1}). For percolated samples the experimental error for conductivities was less than 50%.

For piezoresistive tests, an HP D500 dynamometer coupled with an Arduino Uno microcontroller-based kit was used. A series electrical circuit was built between the Arduino, the sensor (the composite) and a known electrical resistance, applying 5 V. In this way, the sensor was placed in the dynamometer, and the electrical connections were located at the extremes of the sample by clamps serving as electrodes, next to the tension tester grip. This configuration using a surface contact is the standard for strain sensors based on polymer composites.[4] In a similar system, electrodes deposited on the cut edges of the specimen give the same resistivity as electrodes applied on the surfaces.[28] It was therefore concluded that the latter measured resistivity can be a bulk value, although the possibility that it represents a surface resistivity was not eliminated. However, in our case the electrical values from this configuration were much higher than results based on bulk measurements; therefore the electrical conductivity is likely to be by the surface. This system allows the online measurement of the electrical conductivity while the sample is strained by the dynamometer at a rate of 6 mm min^{-1} at 23 °C. For each composite, two samples were tested. The values reported are the relative resistance (RR) defined as the ratio between the resistance of the strained sample divided by the original resistance at zero strain.

RESULTS

Percolation transition

Figure 1 displays the electrical conductivity of the different composites as a function of the filler content showing the effect of both polymer matrix and kind of carbon nanoparticle on the percolation transition. When CNTs were used as filler, composites based on the polymer matrix with a low amount of 1-butene (EB1) displayed a lower percolation threshold compared with those based on the EB2 matrix. For measurements of the concentration threshold, the scaling law from percolation theory was applied to the experimental data:[33]

$$\sigma \propto \left(\phi - \phi_c\right)^t \quad (1)$$

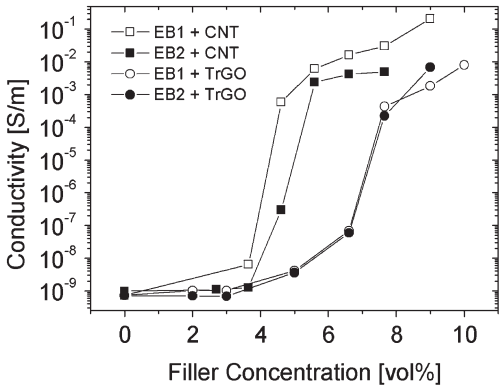

Figure 1. Effect of polymer matrix, carbon nanostructure and filler concentration on the electrical conductivity of the different composites studied.

where σ is the effective electrical conductivity of the composite, ϕ is the filler volume fraction, ϕ_c is the percolation threshold and t is a critical exponent related to the dimensionality of the investigated system. By using this equation, values of 2.4 and 4.6 vol% were found for CNT based composites prepared with EB1 and EB2, respectively. This result can be related to the polymer microstructure as reported previously where an inverse proportion between the percolation threshold and the matrix crystallinity was found in similar systems.[34] Fillers can be dispersed only in the amorphous region of semicrystalline polymer composites as the structure of the crystalline regions is highly compact rejecting the particles. Thus particles usually segregate at the crystal growth fronts.[35,36] For instance, spherical nanoparticles can be considered much larger than the cross-sectional area occupied by polymer chains in the crystal lattice, and their inclusion within the crystal can be considered unlikely.[36] CNTs are therefore expected to be excluded from the polymer during its crystallization, being located in either the gaps between spherulites or the amorphous/boundary regions of lamellar stacks.[35] In this way, the effective concentration of CNTs in the amorphous region is increased with the polymer crystallinity. The same tendency is found in polymer composites having a second non-conductive nanoparticle able to reduce the percolation threshold by decreasing the available volume for CNT dispersion.[37] As expected, independent of the polymer matrix used, CNT composites present a critical exponent t around 5.5. This exponent depends on the system dimensionality with values of 1.33 and 2 for two and three dimensions respectively, based on classical percolation theory.[38] According to percolation theory, the insulator/conductor transition occurs at the critical concentration at which an infinite cluster of connected particles appears. However, in polymer/carbon systems the tunneling effect is a better mechanism explaining that percolation occurs much before particles become physically in contact.[39] This tunnel effect increases the t value fitted experimentally as found in our samples.

On using TrGO as filler, the percolation transition increased compared with CNTs showing the relevance of the carbon nanostructure.[34] The difference is associated with the inverse relationship between the particle aspect ratio and the percolation threshold (see for instance the results from the excluded volume theory below).[39,40] Composites based on TrGO present agglomerates with platelet morphologies and therefore higher thresholds than composites based on CNTs with a tube-like morphology. Composites with TrGO presented a critical exponent t around 4.1

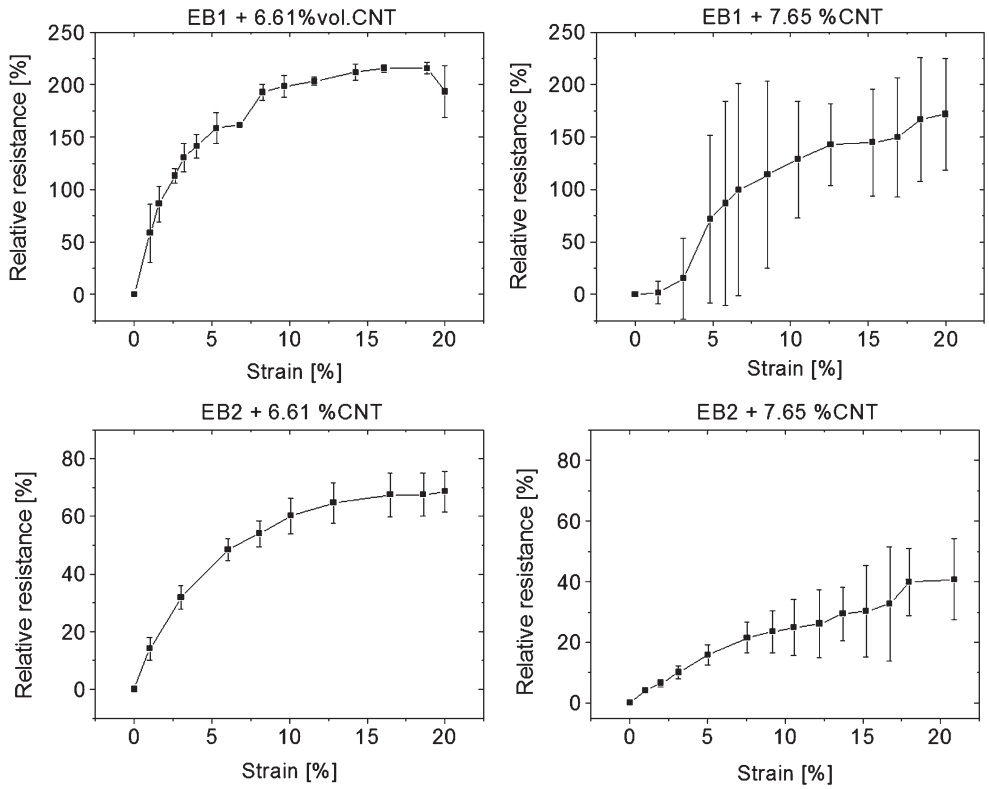

Figure 2. Effect of strain on the relative electrical resistance (RR) of composites based on CNTs.

independent of the polymer matrix, which is lower than composites with CNTs, stressing the effect of carbon nanostructure on the percolation transition. This difference cannot be directly associated with the geometrical information of each filler as even in polymer/CNT composites values between 1.3 and 7 are currently reported.[38] In TrGO composites the effect of the polymer matrix on the percolation transition was barely observed.

Piezoresistive behavior

Based on the information in Fig. 1, composites with 6.6 and 7.6 vol% of CNTs and with 9.0 and 10.0 vol% of TrGO were selected for the piezoresistive tests as they displayed the same percolation levels. In this way, composites both near (6.6 vol% of CNTs and 9.0 vol% of TrGO) and above (7.6 vol% of CNTs and 10.0 vol% of TrGO) the percolation threshold were characterized. Figure 2 displays the effect of strain on the average RR of composites based on CNTs after three cycles, confirming that the electrical resistance is drastically affected by strain. On applying a deformation the resistance increased, i.e. the strain disrupted the CNT percolated network increasing the average interparticle distance.[41] This process is well known in polymer/CNT composites in either the melt or the solid state under different strain conditions.[42] For instance, Kharchenko *et al.* reported flow-induced properties under steady state shear fields in polypropylene/CNT composites above the percolation threshold.[43] They found that the electrical conductivity of the composites decreased several orders of magnitude with the shear rate. This change in conductivity relates to CNT alignment affecting the interparticle distance, as also shown by Winey and colleagues studying polymethylmethacrylate composites in the solid state.[44] The relationship between interparticle distance and electrical conductivity in similar composites has been quantified by the equivalent circuit model where the gaps between either CNT aggregates or CNT/CNT connections were simulated as micro-capacitors and micro-resistors in parallel.[42] High conductive composites presented a minimal distance between particles of 3.4 nm whereas low conductive composites presented a value of 4.0 nm.[42] Moreover, in the melt state these composites displayed a drop in electrical conductivity proportional to the strain applied, confirming that the local elastic deformation suffered by the network of CNTs is the responsible for the changes.

The results from Fig. 2 further show that the sensitivity of the piezoresistive composites is affected by both the polymer matrix and the filler concentration. Regarding the effect of filler concentration, several researchers have stated that composites near the percolation threshold display higher sensitivity than composites at higher concentrations.[4,26] This phenomenon is mainly attributed to the enhancement of conductive networks by increasing the conductive particles.[17] At higher concentrations, the conductive networks become more difficult to disrupt. It was confirmed by atomic force microscopy that, on raising the mass fraction of carbon black in a polymer, the number of conductive channels and therefore the current density were increased.[45] Regarding the matrix effect, composites based on a stiffer matrix (EB1) showed larger piezoresistive sensitivities despite the conclusion from other authors stating that softer polymer matrices produce composites with larger GFs.[11] A comparative study about the effect of the polymer matrix in these systems is difficult as not only the polymers are different but also the filler dispersion. In our case, the stiffer matrix (EB1), having therefore higher elastic modulus, transfers higher stresses to the CNTs and in this way the interparticle distance is more affected than in composites based on EB2 at the same strain. The Cox model for a solid fiber, assuming perfect interfacial bonding, can be extended to CNTs for calculating the interfacial shear stress (τ) along their longitudinal axis.[46] In particular,

at the extremes of the tube where the largest forces appear, the following formulae apply:

$$\tau \propto Et\varepsilon\beta \tanh(\beta K1) \quad (2)$$

$$\beta = [(Gm/Et)K2]^{1/2} \quad (3)$$

where E_t is Young's modulus of the CNTs; ε is the applied strain; G_m is the shear modulus of the matrix (related to its Young's modulus), K_1 and K_2 are constants related to the geometry of the tube, and β is the shear-lag parameter from the Cox model. These equations confirm that, on increasing the modulus of the matrix, the force transferred to the CNTs increases, i.e. greater interparticle distances. A similar tendency was obtained under compression by using a mathematical model for the interparticle distance based on the tunneling effect.[19]

Another result from Fig. 2 is that the standard deviation (SD) of the electrical measurements depends on the filler concentration. After three cycles, composites with high filler concentration present a large SD originating from two phenomena: (1) the high noise of the conductivity reading from the Arduino system at high strain values, and (2) a decrease in the RR as the number of cycles increases. The former phenomenon was mainly observed in the EB1 + 7.6CNT composite, showing the highest conductivity, whereas the latter was mainly observed in the EB2 + 7.6CNT. Variations in the piezoresistive response of the composite with cycles can be explained by non-reversible changes in the agglomeration state of the filler such as strain-induced CNT agglomeration. A non-expected increase in the electrical conductivity of polymer/CNT composites was observed under external strain associated with a decrease in the filler - filler distance.[42] Indeed, after strain the composites can reach a new equilibrium meaning an increase in the electrical conductivity compared with the unstrained sample. Similar results can be found in other systems depending on the agglomeration level of CNTs in the polymer matrix.[47] In our case, the strain applied to the composites could induce a change in the agglomeration state of the CNTs at the end of the cycle, increasing the conductivity and therefore decreasing the RR response of the material in the next cycle. This tendency has been reported previously and was explained by the formation of additional conductive pathways through a breakdown of the polymer - filler interface.[3] These changes in RR with cycles can also be related to a time-dependent mechanical response of the matrix.[12]

Figure 3 shows the effect of tensile strain on RR for composites with TrGO displaying the strong effect of the carbon based nanostructure. While in composites with CNTs the highest RR values were around 250%, in composites with TrGO the RR values reached values as high as 2500%, i.e. an increase by a factor of 10 in sensitivity. Similar to polymer/CNT composites, both a stiffer matrix and samples near the percolation threshold displayed the largest RR values. Under compression, similar changes in the electrical conductivity are generally reported for several polymers with graphite derivative fillers.[17,18,21] For instance, the highest changes were reported for composites closest to the percolation transition as our results confirm (i.e. composites based on EB1). Moreover, on increasing the amount of filler, the RR decreases to values similar to those for composites with CNTs. The general tendency of the curves was also affected by the carbon structure as polymer/CNT composites displayed an asymptotic behavior whereas polymer/TrGO composites displayed an exponential behavior. Moreover, the SDs of sensors based on TrGO were much lower than for those based on CNTs.

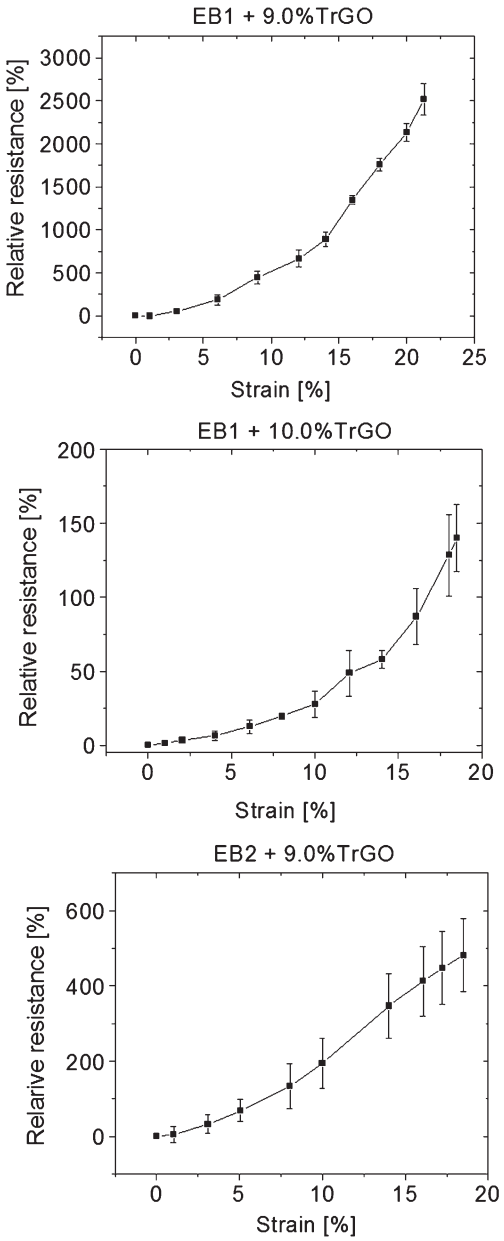

Figure 3. Effect of strain on the relative electrical resistance (RR) of composites based on TrGO.

The effect of filler concentration, carbon nanostructure and polymer matrix is summarized in Fig. 4 plotting the GF for all the samples. In our case, the average GF over the whole range of strain was plotted. Figure 4 shows that the GF was largely affected for the three variables changing from 2 to 55, with the carbon structure being the most relevant variable.

To further understand, at least qualitatively, the effect of both strain and filler concentration, the following model is generally used:[45,48]

$$R = \frac{L}{N}\frac{8\pi hs}{3a^2\gamma e^2}\exp(\gamma s) \quad (4)$$

where R is the resistivity of the composite, L is the number of particles forming a single conducting path, N the number of conducting paths, h Planck's constant, s the least distance between conductive particles, a^2 the effective cross-section where tunneling

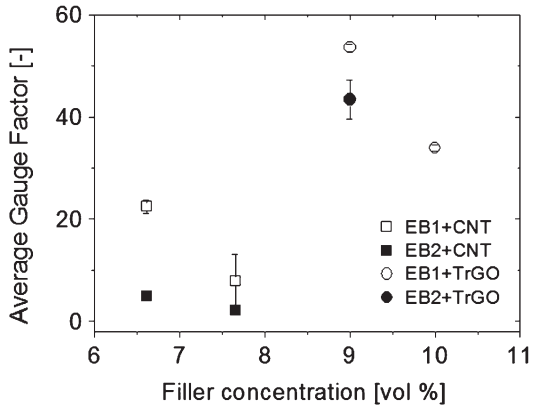

Figure 4. Effect of polymer matrix, carbon nanostructure and filler concentration on the average GF of the different composites studied.

occurs, e the electron charge and γ a constant related to the electron mass and the height of the potential barrier between adjacent particles. By assuming (1) that under an applied stress the sample is deformed by a tensile strain ε and therefore the particle separation changes from s_0 to $s = s_0(1+\varepsilon)$ and (2) that N is not affected by the strain, the RR can be estimated by[45]

$$RR_{N\,Nconst} = \left(\frac{R}{R_0}\right)_{N\ const} = \frac{s_0(1+\varepsilon)}{s_0}\exp\left(\gamma s_0 \varepsilon\right) \tag{5}$$

This expression states that RR is affected by the strain as observed in our samples. However, the effect of the filler concentration cannot be directly concluded from Eqn (5). By adding the effect of changes in N due to the strain ($N(\varepsilon)$) , Eqn (5) becomes

$$RR = \frac{R}{R_0} = \left(\frac{R}{R_0}\right)_{N=const} \cdot \frac{N_0}{N(\varepsilon)} = \left(\frac{R}{R_0}\right)_{N=const} \cdot \frac{N_0}{N_0(1-\delta)} = \left(\frac{R}{R_0}\right)_{N=const} \cdot \frac{1}{(1-\delta)} \tag{6}$$

where N_0 is the number of conducting paths in the unstrained sample and δ is the fraction of particles disconnected from local conduction due to strain.[49] Near the percolation threshold, N_0 is low and any path disrupted by strain will have a significant effect, i.e. high δ values, or low 1 - δ values, and therefore high RR. Therefore, the effect of filler content on the sensitivity of these sensors can be explained by the relative importance of the fraction of disrupted conduction paths.

Analysis applying the excluded volume model

Most of the discussion about the mechanisms explaining the piezoresistive behavior of polymer nanocomposites used an interparticle parameter and its relationship with the tunneling effect, as reported elsewhere.[3,17–19,21,23,45] Hereafter, a different and complementary approach based on the excluded volume theory for percolation transition is developed for a better discussion about our findings. This theory is based on the evidence that the percolation threshold is not linked to the true volume of the object itself but rather to its excluded volume.[50] The excluded volume (V_e) is the volume around an object in which the center of another similarly shaped object is not allowed to penetrate if overlapping of the two objects is to be avoided. In this theory, the invariant property is no longer related to N_cV, where N_c is the critical number density of objects in the system and V is the real volume of the object, but rather to N_cV_e.[51] The total excluded volume $\langle V_{ex}\rangle$ is defined as

$$\langle V_{ex}\rangle = N_c\langle V_e\rangle \tag{7}$$

where $\langle V_e\rangle$ represents the excluded volume of an object averaged over the orientational distribution characterizing the system objects. With these parameters, the relation

$$\phi_c = 1 - \exp\left(-\frac{\langle V_{ex}\rangle V}{\langle V_e\rangle}\right) \tag{8}$$

is applied for the critical concentration at percolation, ϕ_c.[50] $\langle V_{ex}\rangle$ is not a constant although it presents extreme values corresponding to the system characterized by a random orientation (lower limit) or strictly parallel objects (upper limit). The upper limit is the same as the case of permeable spheres. For simplicity, only the lower limit will be used in our analysis, with values of 1.4 and 1.8 for randomly oriented infinitely thin rods (representing CNTs) and disks (representing TrGO), respectively, as reported by Celzard *et al.*[50] One of the main advantages of this approach is the rather easy way to add filler orientation by means of $\langle V_x\rangle$, having values of

$$\langle V_e\rangle = \frac{4\pi}{3}W^3 + 2\pi W^2 L + 2WL^2\langle \sin\gamma\rangle_\mu \tag{9}$$

$$\langle V_e\rangle = r^3\left[2\pi\theta - \pi\sin(2\theta)\right] \tag{10}$$

for rods and disks, respectively. In these equations, W and L represent the diameter and length of the rods having a half-sphere in the ends of diameter $W/2$, whilst r represents the radius of the disk; $\langle \sin\gamma\rangle_\mu$ is a parameter related to the average angles of two rods in contact with each other, with a value of $\pi/4$ for randomly oriented systems, decreasing for more oriented fillers, and θ represents the angle of greatest disorientation of the disks with a value of $\pi/2$ for randomly oriented systems. Based on these equations, the concentration threshold of composites based on fillers with different aspect ratios and orientations is estimated as

$$\phi_c = 1 - \exp\left(-\frac{1.4\left[(\pi/4)W^2L + (\pi/6)W^3\right]}{\frac{4\pi}{3}W^3 + 2\pi W^2 L + 2WL^2\sin\gamma_\mu}\right) \tag{11}$$

$$\phi_c = 1 - \exp\left(-\frac{1.8\pi r^2 t}{r^3(2\pi\theta - \pi\sin(2\theta))}\right) \tag{12}$$

for rods and disks, respectively, where t is the thickness of the disk. Moreover, with these equations the average number of objects connected to a given particle, B_c, can be roughly estimated. This parameter arises from continuum percolation providing information on the local topology of the percolating cluster. For fully penetrable objects the value is[52]

$$B_c = \rho_c \cdot V_e = \frac{\phi_c}{V}V_e \tag{13}$$

where ρ_c is the number density at percolation and V_e and V are the excluded and the total volume, respectively, of the filler.

This model takes into account the strong effect of the particle aspect ratio, giving percolation transitions at 1.9 vol% and 5.2 vol% for CNTs and TrGO, respectively, with values of $L = 500$ nm and $W = 15$ nm for CNTs and $r = 1600$ nm and $t = 250$ nm for TrGO. These values are a good approximation considering the unknown real morphology of the particles which is rather complex with

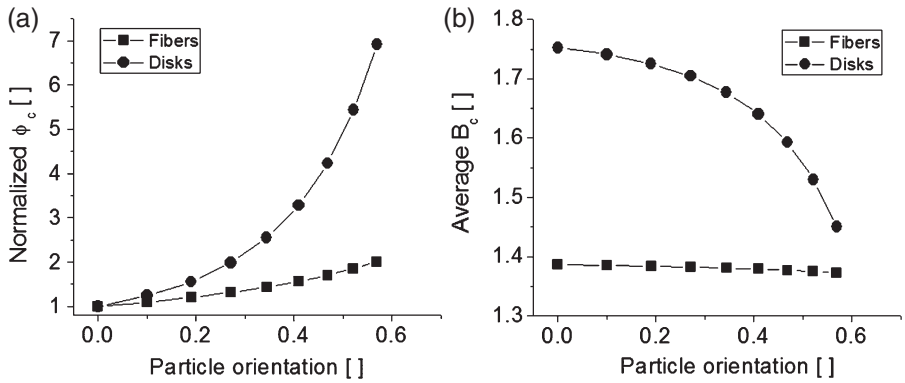

Figure 5. Effect of particle aspect ratio and deformation angle on (a) the normalized percolation threshold and (b) the average number of objects connected to a given particle, measured according to the excluded volume theory.

different degrees of agglomeration through the polymer. With these values, the average number of bonded objects per given object (B_c) was 1.38 and 1.75 for composites with CNTs and TrGO, respectively.

Regarding the piezoresistive behavior of the samples, these equations can be used assuming that the strain in polymer nanocomposites produces a change in the orientation of the particles. This strain orientation is well reported in polymer/CNT composites by means of the relationship between interparticle distance (s), further depending on the strain (ε) and particle orientation:[23]

$$s = s_0 \left[1 + \varepsilon \left(\cos^2\theta_p - \nu \sin^2\theta_p\right)\right] \quad (14)$$

where υ is Poisson's ratio of the matrix, s_0 is the initial interparticle distance and θ_p is the particle orientation. A similar relationship can be found between the fiber strain and its orientation.[53,54] Hereafter, we assume that strain affects the orientation of the different carbon based nanoparticles by changing $\langle \sin\gamma \rangle_\mu$ (Eqn (9)) and $\sin\theta$ (Eqn (10)) for CNTs and TrGO, respectively. This strain based filler orientation will affect the critical percolation threshold (Eqns (11) and (12)) and therefore the overall conductivity of the composites. To facilitate the discussion based on the excluded volume theory, we simply define orientation as 1 - angle/(π/4) and 1 - angle/(π/2) for CNTs and TrGO, respectively, having a value of zero for randomly oriented particles (unstrained system) and increasing as the angle decreases (oriented particles). Figure 5 displays the effect of this orientation parameter on the concentration threshold (Eqns (11) and (12)) for the different carbon nanostructures studied showing the strong effect of the particle aspect ratio. While composites with CNTs were barely affected by orientation, composites with TrGO drastically increased the transition threshold. These results agreed with the tendency found in Figs 3 and 4 regarding the effect of particle aspect ratio on the strain sensitivity of the composites. Figure 5 also confirms that the effect of carbon morphology is related to a decrease in the number of connected fillers in the conduction paths as concluded by analyzing B_c. These results showed that the excluded volume is able to explain the effect of the particle aspect ratio on both the percolation transition and the sensitivity of piezoresistive materials. However, it is relevant to point out that, although the excluded volume theory can be used to predict the percolation threshold in composites with fillers of any aspect ratio, it is particularly efficient in systems possessing large aspect ratio particles.[48] In particular, our analysis based on the orientation of particle fillers for predicting the piezoresistive behavior of composites is limited to non-spherical particles.

CONCLUSIONS

The electrical behavior, for instance the percolation transition and the piezoresistivity, of polymer composites based on carbon nanostructures can be tailored by changing the matrix, the filler concentration and the particle aspect ratio. In particular, composites with TrGO displayed much more strain sensitivity than those with CNTs, with differences as great as one order of magnitude. In particular, the mechanical properties of the matrix and the proximity to the percolation threshold were relevant variables affecting the electrical dynamics of the composites. The excluded volume theory for percolated systems was able to support our main results regarding the effect of particle aspect ratio on the piezoresistive behavior of these composites.

ACKNOWLEDGEMENTS

We thank the Comisión Nacional de Investigación Científica y Tecnológica (CONICYT) for the financial support from Projects Fondecyt No. 1150130. The support of Mario Vergara, Chief of the Electrical Testing Unit, Instituto de Investigaciones y Ensayos de Materiales (IDIEM) from the University of Chile, is also acknowledged.

REFERENCES

1 Moniruzzaman M and Winey KI, *Macromolecules* **39**:5194-51205 (2006).
2 Araby S, Meng Q, Zhang L, Zaman I, Majewski P and Ma J, *Nanotechnology* doi:10.1088/0957-4484/26/11/112001 (2015).
3 Ji M, Deng H, Yan D, Li X, Duan L and Fu Q, *Compos Sci Technol* **92**:16–26 (2014).
4 Pham GT, Park YB, Liang Z, Zhang C and Wang B, *Compos B* **39**:209–216 (2008).
5 Costa P, Silva J, Ansón-Casaos A, Martinez MT, Abad MJ, Viana J *et al.*, *Compos B* **61**:136–146 (2014).
6 Slobodian P, Riha P and Saha P, *Carbon* **50**:3446-3453 (2012).
7 Lu N, Lu C, Yang S and Rogers J, *Adv Funct Mater* **22**:4044-4050 (2012).
8 Yamada T, Hayamizu Y, Yamamoto Y, Yomogida Y, Izadi-Najafabadi A, Futaba DN *et al.*, *Nat Nanotechnol* **6**:296-301 (2011).
9 Li X, Zhang R, Yu W, Wang K, Wei J, Wu D *et al.*, *Sci Rep* **2**: 870 (6 pages) (2012).
10 Chun S, Kim Y, Jin H, Choi E, Lee SB and Park W, *Carbon* **78**:601-608 (2014).

11 Costa P, Silvia C, Viana JC and Mendez SL, *Compos B* **57**:242–249 (2014).
12 Zhang R, Deng H, Valenca R, Jin J, Fu Q, Bilotti E *et al.*, *Compos Sci Technol* **74**:1–5 (2013),
13 Georgousis G, Pandis C, Kalamiotis A, Georgiopoulos P, Kyritsis A, Kontou E *et al.*, *Compos B* **68**:162–169 (2015).
14 Lin L, Liu S, Zhang Q, Li X, Ji M, Deng H *et al.*, *ACS Appl Mater Interfaces* **5**:5815-5824 (2013).
15 Geim K and Novoselov KS, *Nat Mater* **6**:183–191 (2007).
16 Qu S and Wong SC, *Compos Sci Technol* **67**:231–237 (2007).
17 Lu J, Chen X, Lu W and Chen G, *Eur Polym J* **42**:1015–1021 (2006).
18 Lu J, Weng W, Chen X, Wu D, Wu C and Chen G, *Adv Funct Mater* **15**:1358-1363 (2005).
19 Chen G, Lu J, Lu W, Wu D and Wu C, *Polym Int* **54**:1689-1693 (2005).
20 Chen L, Chen G and Lu L, *Adv Funct Mater* **17**:898-904 (2007).
21 Al-solamy FR, Al-Ghamdi AA and Mahmoud WE, *Polym Adv Technol* **23**:478-482 (2012).
22 Kumar SK, Castro M, Saiter A, Delbreilh L, Feller JF, Thomas S *et al.*, *Mater Lett* **96**:109–112 (2013).
23 Wichmann MHG, Buschhorn ST, Gehrmann J and Schulte K, *Phys Rev B* **80**:245437 (2009).
24 Hu N, Karube Y, Arai M, Watanabe T, Yan C, Li Y *et al.*, *Carbon* **48**:680-687 (2010).
25 Knite M, Teteris V, Polyakov B and Erts D, *Mater Sci Eng C* **19**:15-19 (2002).
26 Hu N, Karube Y, Yan C, Masuda Z and Fukunaga H, *Acta Mater* **56**:2929-2936 (2008).
27 Bensason S, Minick J, Moet A, Chum S, Hiltner A and Baer E, *J Polym Sci B Polym Phys* **34**:1301-1315 (1996).
28 Flandin L, Hiltner A and Baer E, *Polymer* **42**:827-838 (2001).
29 Flandin L, Chang A, Nazarenko S, Hiltner A and Baer E, *J Appl Polym Sci* **76**:894-905 (2000).
30 Eynde SV, Mathot V, Koch MHJ and Reynaers H, *Polymer* **41**:3437-3453 (2000).
31 Hummers W and Offeman R, *J Am Chem Soc* **80**:1339-1339 (1958).
32 Garzon C and Palza H, *Compos Sci Technol* **99**:117–123 (2014).
33 Stauffer D and Aharony A, Introduction to Percolation Theory, *2nd revised edn*. Taylor and Francis: London, 2003.
34 Li YJ, Xu M, Feng JQ, Cao XL, Yu YF and Dang ZM,*J Appl Polym Sci* **106**:3359-3365 (2007).
35 Xu D and Wang Z, *Polymer* **49**:330-338 (2008).
36 Waddon AJ and Petrovic ZS, *Polym J* **34**:876-881 (2002).
37 Palza H, Garzón C and Arias O, *eXPRESS Polym Lett* **6**:639-646 (2012).
38 Bauhofer W and Kovacs JZ, *Compos Sci Technol* **69**:1486-1498 (2009).
39 Linares A, Canalda JC, Cagiao ME, Garcia-Gutierrez MC, Nogales A, Martin-Gullon I *et al.*, *Macromolecules* **41**:7090-7097 (2008).
40 Yi JY and Choi GM, *J Electroceram* **3-4**:361-369 (1999).
41 Alig I, Lellinger D, Dudkin SM and Pötschke P, *Polymer* **48**:1020-1029 (2007).
42 Palza H, Kappes M, Hennrich F and Wilhelm M, *Compos Sci Technol* **71**:1361-1366 (2011).
43 Kharchenko SB, Douglas JF, Obrzut J, Grulke EA and Migler KB, *Nat Mater* **3**:564-568 (2004).
44 Du F, Fischer JE and Winey KI, *Phys Rev B* **72**:121404 (2005).
45 Knite M, Teteris V, Kiploka A and Kaupuzs J, *Sens Actuators A Phys* **110**:142–149 (2004).
46 Xiao KQ and Zhang LC, *J Mater Sci* **39**:4481-4486 (2004).
47 Bauhofer W, Schulz SC, Eken AE, Skipa T, Lellinger D, Alig I *et al.*, *Polymer* **51**:5024-5027 (2010).
48 Zhang XW, Pan Y, Zheng Q and Yi XS, *J Polym Sci B* **38**:2739-2749 (2000).
49 Angelidis N, Wei CY and Irving PE, *Compos A Appl Sci Manuf* **35**:1135-1147 (2004).
50 Celzard A, McRae E, Deleuze C, Dufort M, Furdin G and Mareche JF, *Phys Rev B* **53**:6209-6214 (1996).
51 Balberg I, Anderson CH, Alexander S and Wagner N, *Phys Rev B* **30**:3933-3943 (1984).
52 Ambrosetti G, Johner N, Grimaldi C, Danani A and Ryser P, *Phys Rev E* **78**:061126 (2008).
53 Cooper CA, Young RJ and Halsall M, *Compos A Appl Sci Manuf* **32**:401-411 (2001).
54 Wood JR, Zhao Q and Wagner HD, *Compos A Appl Sci Manuf* **32**:391-399 (2001).

